Research Journal of Applied Sciences 3 (4): 317-323, 2008
ISSN: 1815-932X

Rapid Coagulation/Flocculation Kinetics of Coal Effluent with High Organic Content Using Blended and Unblended Chitin Derived Coagulant (CSC)

[1]M.C. Menkiti, [1]P.K. Igbokwe, [1]F.X.O. Ugodulunwa and [1]O.D. Onukwuli
[1]Department of Chemical Engineering, Nnamdi Azikiwe University, Awka, Nigeria
[2]Department of Geology and Mining University of Jos, Nigeria

Abstract: The coagulation performance of crab shell coagulant (CSC) using coal washery effluent has been investigated at room temperature using various dosages of blended and unblended CSC. In addition, the coagulation reaction rate constant, K, the order of reaction, α and the distribution of particles were also determined. Turbidity measurement was employed using the nephelometric (turbidimetric) standard method. The least and highest values for order of reaction (α) recorded are 0.9 and 6 while that of reaction constant (K) are 1.6618×10^{-19} L g min^{-1} and 6.6823×10^{-2} min^{-1}, respectively. The best turbidity removal occurred for 400 mg L^{-1} Alum + 100 mg L^{-1} $FeCl_3$ and 400 mg L^{-1} CSC. With the exception of few, the computed order of reaction agrees with the results of previous workers. The results obtained confirmed that the theory of fast coagulation holds for the coagulation of the coal washery effluent using the coagulants investigated and at the conditions of the experiment.

Key words: Coagulation, kinetics, turbidity, coal washery effluent, floc, flocculation, nephelometry

INTRODUCTION

Coagulation and flocculation processes are of practical importance in waste water treatment. Traditionally, the coagulation process is described in terms of the destabilization of colloids initially present in water supply (Ma *et al*., 2001). The destabalised colloids overcome their repulsive forces leading to the aggregation of the particles to form flocs (Di Terlizzi, 1994; Edzwald, 1987; O'Melia, 1978).

To remove colloidal materials, a floc forming chemical is needed to sweep off the suspended colloidal material and as much of the solute as possible.

There are numerous factors that influence coagulation/flocculation process such as raw water quality, temperature, chemical and bacteriological parameters, treatment device structure as well as coagulant types and dosages (Jin, 2005).

Coagulation/flocculation of waste water may be accomplished with any of the common water coagulants including lime, iron and aluminum salts and synthetic polymers. The coagulation performance and behaviour of these common coagulants/flocculants have been well investigated by means of nephelometry with little or no attention given to the coagulation potential of many animal and plant derivatives. To this end, a focus is hereby given to the study on crab shell as a potential source of coagulant derivative. Crab shell is a natural carbohydrate bipolymer derived by deacetylation of chitin, a major component of the shells of crustacean such as crab, shrimps and crawfish (Fernandez-Kim, 2004).

Crab shell coagulant (CSC) is a non-toxic, biodegradable and bicompatible polymer. Previous results obtained from the study on crustacean derived coagulants highlight promising renewable polymeric materials with extensive application in removal of colloidal particles in wide range of effluent media (Fernandez-Kim, 2004).

However, in spite of the abundance of crabs in our local communities in Nigeria, little or no comprehensive work has been reported. Against this backdrop, this work endeavours to explore and generate interest in the utilization of crab shell as coagulants. The work embraces some aspect of coagulation performance, kinetics and mechanism associated with coagulation of coal washery effluent using CSC and it blends with $FeCl_3$ and alum. Thus, if well developed, CSC can serve as a suitable replacement either in total or in part for the polyelectrolytes and synthetic coagulants that are not only costly but environmentally unfriendly.

MATERIALS AND METHODS

The experimental procedures were conducted based on international Bench Scale Jar test and Standard

Corresponding Author: P.K. Igbokwe, Department of Chemical Engineering, Nnamdi Azikiwe University, Awka, Nigeria

Nephelonometric Method for the examination of water and wastewater (WST, 2005; AWWA, 2005; APHA, 2005; Greenberg, 1992; Bagwell *et al*., 2001; JAWWA, 1985).

Theoretical principles and model development: The kinetics of Brownian coagulation of monodispersed particles at the early stage is described generally by:

$$\frac{dC}{dt} = -KC^{\alpha} \quad (1)$$

Taking in of Eq. 1 gives:

$$In\left(\frac{-dC}{dt}\right) = InK + \alpha InC \quad (2)$$

From which K and α can be determined from a plot of:

$$In\left(\frac{-dC}{dt}\right) \text{ vs } InC.$$

where,

K = Coagulation rate constant/collision frequency/ Absolute coagulation rate constant.
α = The order of coagulation reaction.
C = The concentration of the particles (TSS).

It has been shown by many workers that for the conditions described above (Fridrikhsberg, 1984; Van-Zanten and Elimelechi, 1992; Smoluchowski, 1917).

$$K = 8\pi R^{l} D$$
$$\alpha = 2 \quad (3)$$

$$R^{l} = 2a \quad (4)$$

where,

a = Particle radius.
D = Diffusivity.

From Einstein's Equation (Fridrikhsberg, 1984; Danov *et al*., 2001):

$$D = K_B T/B. \quad (5)$$

where,

B = The friction factor.
T = Absolute temperature (°K).
K_B = The Boltzman constant (molar gas constant per particle).

For the simplest case of a smooth spherical particle of radius a, immersed in a fluid of viscosity η, B is given by the stokes relation (Fridrikhsberg, 1984):

$$B = 6\pi\eta\alpha \quad (6)$$

Putting Eq. 6 into 5 gives:

$$D = \frac{K_B T}{6\pi\eta a} \quad (7)$$

But R = 2a

$$\therefore D = \frac{2K_B T}{6\pi\eta R^{1}} = \frac{K_B T}{3\pi\eta R^{1}} \quad (8)$$

Putting Eq. 8 into 3 gives:

$$K = 8\pi R^{1}\left[\frac{K_B T}{3\pi\eta R^{1}}\right]$$
$$K = \frac{8}{3}\frac{K_B T}{\eta} \quad (9)$$

Putting Eq. 9 into 1 yields:

$$\frac{dC}{dt} = -\frac{8}{3}\frac{K_B T}{\eta}C^{2} \quad (10)$$

Applying the method of separable variable and integrating Eq. 1 within the following limits:

$$\text{At } t = 0,\ C = C_o$$
$$\text{At } t = t,\ C = C$$

yields:

$$-\frac{dC}{C^{2}} = Kdt \quad (11)$$

$$\int_{c_0}^{c} C^{-2}dC = \int_{o}^{t} Kdt \quad (12)$$

$$\frac{1}{C} = \frac{1}{C_o} + Kt \quad (13)$$

Multiply both sides of Eq. 13 by C_o to give:

$$\frac{C_o}{C} = \frac{1}{1} + C_o Kt \quad (14)$$

Making C the subject yields:

$$C = \frac{C_o}{1 + C_o Kt}$$

$$\frac{C_o}{1+\frac{t}{\left(1/C_oK\right)}} \quad (15)$$

$$\text{Let } (1/C_oK) = \tau \quad (16)$$

∴Eq. 15 becomes:

$$C = \frac{C_o}{1+\frac{t}{\tau}} \quad (17)$$

when, t = τ, then Eq. 17 becomes:

$$C = \frac{C_o}{1+1} = \frac{C_o}{2} \quad (18)$$

Thus at t =τ; C= C_O/2. This quantity is called the coagulation period, which is the time during which the initial concentration of particles is halved.

It has also been shown that for Brownian coagulation of monodispersed particles at early stage (t≤30 min); the time evolution of the cluster-size distribution for colloidal particle is usually described:

$$\frac{dC_n}{dt} = \frac{1}{2}\sum_{i+j=n} K_{ij}C_iC_j - C_N\sum_{i=1}^{\infty}K_{in}C_i \quad (19)$$

where,

$C_{n(t)}$ = The time-dependent number concentration of n-fold clusters.

t = The time.

K_{ij} = The elements of the rate kernel which control the rate of coagulation between an i - fold and j - fold cluster.

By assuming a constant kernel. i.e.,

$$K_{ij} = K = \frac{8}{3}\frac{K_BT}{\eta}$$

Eq. 19 can be solved exactly, resulting in the expression (Holthof *et al*., 1996):

$$\frac{C_{n(t)}}{C_o} = \frac{\left(K_{11}C_o\,t/2\right)^{n-1}}{\left(1+K_{11}C_o\,t/2\right)^{n+1}} \quad (20)$$

$$\frac{C_{n(t)}}{C_o} = \frac{\left[t/2\left(\frac{1}{KC_0}\right)\right]^{n-1}}{\left[1+t/2\left(\frac{1}{KC_0}\right)\right]^{n+1}} \quad (21)$$

Recall from Eq. 16, τ = ($1/C_O$.k). Put Eq. 16 in 21:

$$\frac{C_{n(t)}}{C_o} = \frac{\left[t/2\tau\right]^{n-1}}{\left[1+t/2\tau\right]^{n+1}} \quad (22)$$

Let, 2τ = τ′ and put in Eq. 22:

$$\frac{C_{n(t)}}{C_o} = \frac{\left[t/\tau'\right]^{n-1}}{\left[1+t/\tau'\right]^{n+1}} \quad (23$$

Equation 23 gives general expression for particle of any ith order. Hence,: for primary particles, (i = 1):

$$C_i = C_o\left[\frac{1}{\left(1+t/\tau'\right)^2}\right] \quad (24)$$

for twins (i = 2):

$$C_2 = C_o\left[\frac{\left(t/\tau'\right)^1}{\left(1+t/\tau'\right)^3}\right] \quad (25)$$

for triplets (i = 3):

$$C_3 = C_o\left[\frac{\left(t/\tau'\right)^2}{\left(1+t/\tau'\right)^4}\right] \quad (26)$$

The process of aggregation is a complicated phenomenon. Analysis shows that Eq. 17 holds for the overall concentration of all particles, which monotonically decreases in time like the number of primary particles:

$$\sum C_i = \frac{C_o}{1+t/\tau'} \quad (27)$$

Linearising Eq. 27 gives:

$$\frac{1}{\sum C_i} = \frac{1}{C_o} + \frac{1}{\tau' C_o}t \quad (28)$$

where,a plot of $1/\Sigma C_i$ versus t produces:

$$\text{Slope} = 1/\tau C_O$$

$$\text{Intercept} = 1/C_O$$

Note that τ can be obtained from slope of Eq. 28 while, the theoretical quantities τ are found with aid of Eq. 16 (Fridrikhsberg, 1984):

$$\tau = \frac{1}{C_o.K} = \frac{3\eta}{8K_B TC_o} \quad (29)$$

As $C_o \rightarrow C_o/2$, $\tau \rightarrow t_{½}$

$$\therefore t_{½} = \frac{3}{8}\frac{\eta}{K_B T(0.5C_o)} = \frac{3}{4}\frac{\eta}{K_B TC_o} \quad (30)$$

where,

$t_{½}$ = is coagulation time/half life

In the work of Holthof *et al.* (1996), it was shown that the coagulation rate constant could be determined by monitoring the changes in the turbidity of the coagulation liquid with time. The particle concentration during early stages of coagulation can be determined directly, by visual particle counting or indirectly, from turbidity (spectrophotometric of light scattering) measurement (Nicholls,1979).

Hence, it is usual to restrict measurement to the early stages (say t≤30 min) of coagulation (where the early aggregation mechanism is most straight forward (Ma *et al.*, 2001,WST, 2005; Van-Zanten and Elimelechi, 1992; Holthof *et al.*, 1996; Metcalf and Eddy, 2003).

Based on the work of Metcalf and Eddy (2003), the relationship between turbidity and Total suspended solid is:

$$TSS\ (mg\ L^{-1}) = (TSS_f).\ T \quad (31)$$

where,

TSS = Total suspended solid.

(TSS_f) = Factor used to convert turbidity reading (NTU) to TSS (mg L^{-1}).

RESULTS AND DISCUSSION

Jar test results: The results obtained in the Unit of Turbidity (NTU) were converted to concentrations (mg L^{-1}) by multiplying by a factor of 2.35 (Nicholls, 1979). These results (concentration units only) are presented in Fig. 1 and 2. The initial concentration, C_o is 4250 mg L^{-1}.

The general trend in Fig. 1 and 2 is that the turbidity decreases with time. The highest degree of coagulation was witnessed with the first 5 min. For the runs indicated in Fig. 1 and 2, nearly or more than half of the coagulation takes place within the first 5 min. This indicates that in the real terms, the coagulation process monitored in this research, has a half life in the region of 5 min.

The decrease of turbidity with time reflects the fact that as the reaction proceeds, the amount of particle available for the coagulation decreases. The sharp decrease in turbidity between 0 and 5 min is a product of either floc sweep mechanism of or combination of entrapment-bridging mechanism (WST, 2005).

Figure 1 shows that the coagulation occurred for the blend of 400 mg L^{-1} Alum + 100 mg L^{-1} CSC. The least coagulation occurs for the blend of 500 mg L^{-1} Alum + 100 mg L^{-1} CSC. The result is expected if it is observed from Fig. 1 that the least turbidity at 5 min time occurred for 400 mg L^{-1} Alum + 100 mg/ CSC. This is due to the ability of Alum to initiate particle sweep. The decrease at blend of 500 mg L^{-1} + 100 mg L^{-1} CSC may be attributed to the ability of alum to re-turbidize effluent when at excess.

It was also evident from Fig. 2 that best coagulation occurred for the CSC dosage of 400 mg L^{-1}. The least particle removal occurred at CSC dosage of 200 mg L^{-1}. The information from Fig. 2 indicates that the probability of re-turbidization setting in is high at dosage being greater than 400 mg L^{-1}.

In general note, the sharp reduction in TSS observed in Fig. 1 and 2 is in accordance with the theory of fast coagulation proposed by Smoluchowski (1917). This supports the real life application of coagulation in which 90% TSS removal is usually achieved within the first 5 min (WST, 2005).

Coagulation reaction constants: The values obtained for the reaction constants are shown in Table 1 and 2. Table 1 presents the values of K, τ, τ′, (-r) and α for the blended CSC while Table 2 presents for the varying unblended doses of CSC. It should be stated that the values of K and α are determined from equations determined from linearized plots of Fig. 3 and 4. The slope gives the value of α while the value of K is determined from the intercepts.

The values of K in Table 1 and 2 show that the least values of K is 1.6618×10^{-19} $l^5\ g^{-5}$ min while, the highest is 2.7824×10^{-4} L g min^{-1}. This shows that the blends with very high values of α maintain low values of K. As the values of α decreases, the value of K tends to increase. The relationship observed between α and K is expected. Since K, is basically rate per concentration and K is

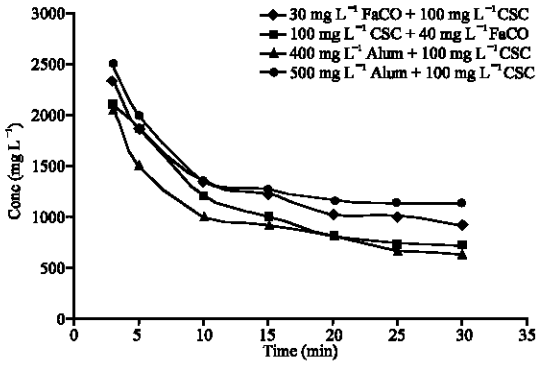

Fig. 1: Particle conc (mg L^{-1}) vs time for blended CSC

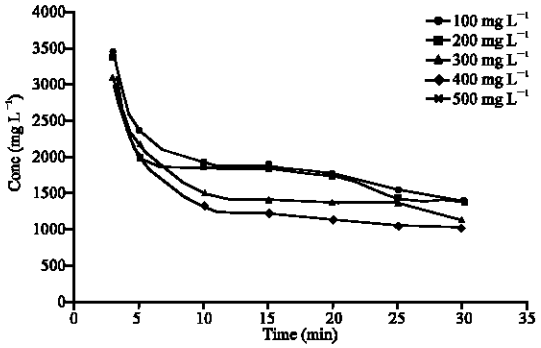

Fig. 2: Particle conc (mg L^{-1}) vs time (min) varying unblended CSC dosages

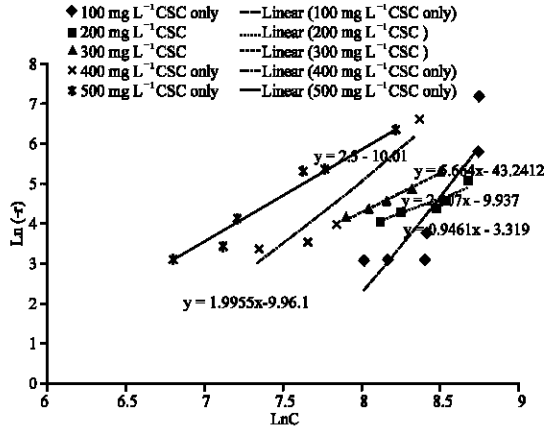

Fig. 3: Polt of ln (-r) vs in C for varying unblended CSC dosages

associated with energy barrier, (KT), it is understandable that for higher α to be obtained, a lower K is a necessary condition for that (Fridrikhsberg, 1984).

The values of K and α obtained in this research, are consistent with previous studies of Brownian coagulation (Fernandez-Kim, 2004; Smoluchowski, 1917). The ranges

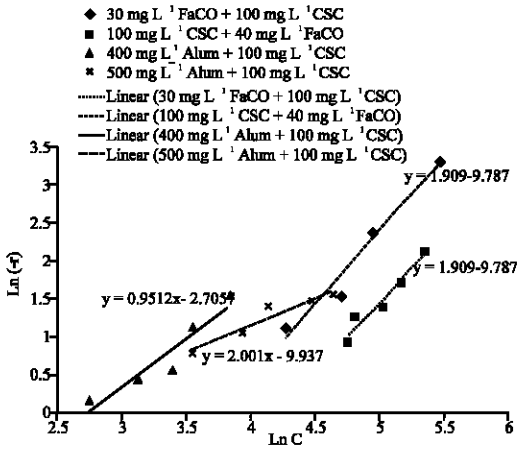

Fig. 4: Polt of ln (-r) vs in C for blended CSC dosage

of α are between 0.9 and 6. With the exception of 0.9 and 6, the result is consistent with the theory of Smoluchoski, which is the foundation of Browinan control coagulation (Fridrikhsberg, 1984; Metcalf and Eddy, 2003). However, any discrepancy in the expected corresponding behaviour between α and K could be attributed to the retarding effect of hydrodynamic interaction (Fernandez-Kim, 2004) which is not accounted for in Brownian coagulation.

Also presented in Table 1 and 2 are the values of τ and τ′. The values of τ′ has a significant effect on the behaviour of the particle distribution of any coagulation process. High value of τ′ favours charge neutralization dominated mechanism. This is shown in the curves of Fig. 5 and 6. However, low value of τ′ favours colloidal entrapment that leads to floc sweep as shown in Fig. 7 and 8.

Particle distribution behaviour: The particle distribution of the coagulation process is presented here. The distribution behaviour is presented in the graphical form of concentration versus time. The particle distribution can be denoted by C_i where C stands for concentration and subscripts i stands for 1, 2, or 3. For primary particles, i = 1, for secondary i = 2 and for triplets, i = 3. The singlets are composed of monomers while doublets are composed of double monomers. Finally, the triplets are composed of 3 monomers.

The particle distribution plots principally show the pattern and distribution of aggregation of ions/particles as they floc into visible blobs. The discussion is presented in 2 cases as follows:

Case I: From Fig. 5 and 6 it is evident that the distribution of particles expected in typical coagulation process is shown here. The curves are for 400 mg L^{-1} CSC only and

Table 1: Coagulation Parameters for the blended CSC

Coagulant (s)	K	α	Rate equation	τ (min)	τ^{1} (min)
30 mg L^{-1} $FeCl_3$ + 100 mg L^{-1} CSC	5.617×10^{-5} L g min^{-1}	2.2	$-r = 5.6\times10^{-5}$ C^2	4.1889	8.3779
40 mg L^{-1} $FeCl_3$ + 100 mg L^{-1} CSC	2.7824×10^{-4} L g min^{-1}	2.0	$-r = 2.7\times10^{-4}$ C^2	0.8456	1.6913
500 mg L^{-1}Alum + 100 mg L^{-1} CSC	6.6823×10^{-2} i min^{-1}	1.0	$-r = 6.6\times10^{-2}$ C^1	3.5×10^{-3}	7×10^{-3}
400 mg L^{-1}Alum + 100 mg L^{-1} CSC	4.835×10^{-5} L g min^{-1}	1.0	$-r = 4.8\times10^{-5}$ C^2	4.8664	9.7329

Table 2: Coagulation Parameter for the varying unblended CSC

Coagulant (s)	K	α	Rate equation	τ	τ^{1}
100 mg L^{-1} CSC only	1.6618×10^{-19} L g min^{-1}	6.0	$-r = 1.6\times1019$ C^6	1.4×10^{15}	2.8×10^{15}
200 mg L^{-1} CSC only	3.6189×10^{-2} L g^{-1} min	0.9	$-r = 3.6\times10^{-2}$ $C^{0.9}$	6.5×10^{-3}	0.0130
300 mg L^{-1} CSC only	4.8352×10^{-5} L g min^{-1}	2.0	$-r = 4.8\times10^{-5}$ C^2	4.86622	9.7325
4000 mg L^{-1} CSC only	4.6312×10^{-5} L g min^{-1}	2.0	$-r = 4.6\times10^{-5}$ C^2	5.0806	10.1612
500 mg L^{-1} CSC only	4.4858×10^{-5} L g min^{-1}	2.0	$-r = 4.4\times10^{-5}$ C^2	5.2453	10.4906

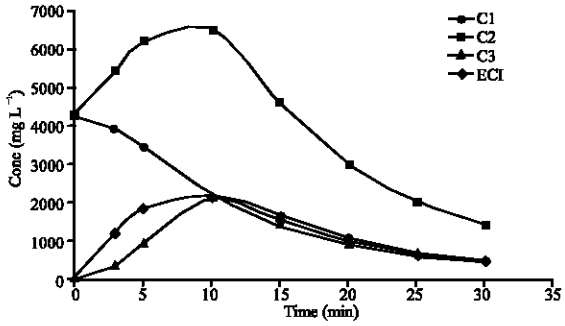

Fig. 5: Particle distribution Polt for 400 mg L^{-1} CSC only

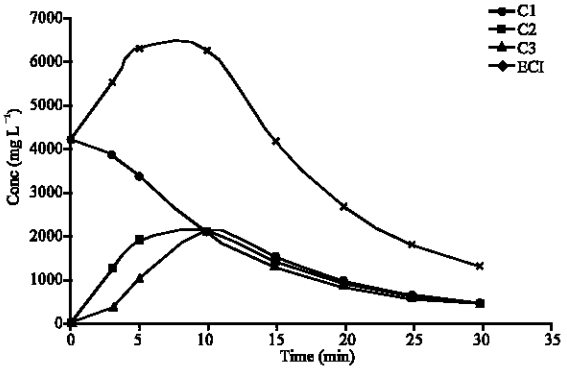

Fig. 6: Particle distribution Polt for 400 mg L^{-1} Alum + 100 mg L^{-1} CSC

400 mg L^{-1} Alum + 100 mg L^{-1} CSC. These curves are expected in coagulation where there is absence of colloidal entrapment and high shear resistance. Mainly, the dominant mechanism in the graph is charge neutralization combined with low bridging to ensure moderate speed of coagulation as represented by both graphs. The discrete nature of formation of C_1, C_2 and C_3 is also associated with low energy (Lentech, 2005).

Case II: From Fig. 7 and 8 showing the particle distribution for 200 mg L^{-1} CSC and 40 mg L^{-1} $FeCl_3$+

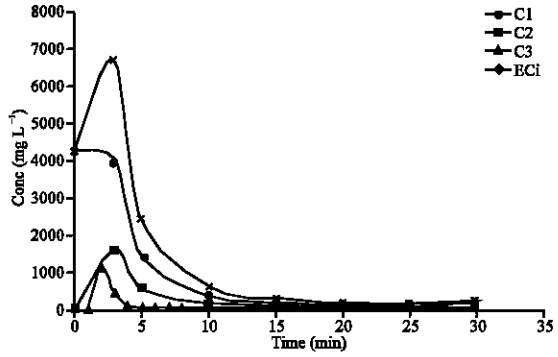

Fig. 7: Particle distribution Polt for 200 mg L^{-1} CSC only

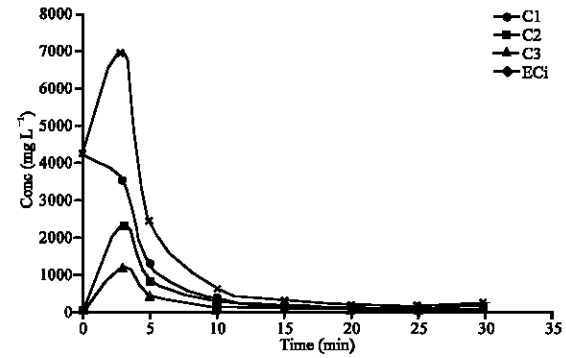

Fig. 8: Particle distribution Polt for 40 mg L^{-1} $FeCl_3$ + 100 mg L^{-1} CSC

100 mg L^{-1} CSC, there is apparent sharp decrease in C_1 between time 0 and 5 min. This type of distribution indicates that the controlling mechanism in the coagulation process is colloidal entrapment that leads to floc sweep as represented by Fig. 7 and 8.

CONCLUSION

The reduction of TSS recorded within the first 5 min of coagulation presents the potential of CSC as a chitin derived coagulant that can be applied in large scale water treatment.

The experimental result with respect to K and α highly agreed with the works of Jin (2005), Holthof (1996) and Van Zanten and Elimelechi (1992).

Jar test in conjunction with nephelometric method still provide routine and convenient means of conducting flocculation and coagulation studies.

Nomenclature:

TSS : Total Suspended Solid.
CSC : Crab Shell Coagulant.
(-r) : rate of depletion of TSS.
Co : Initial Concentration of TSS is effluent.
NTU : Nephelometric Turbidity Unit.

REFERENCES

American Public Health Association (APHA), 2005. Standard Methods for the Examination of Water Effluent, New York, U.S.A.

American Water Works Association (AWWA), 2005. Standard Methods for the Examination of Water Effluent, New York, U.S.A.

Bagwell, T., H.B. Henry and M.B. Kenneth, 2001. Handbook of Public Water System. 2nd Edn. HDR Engineering Inc. New York.

Danov, D.K., P.A. Kralchevsky and I.B. Ivanov, 2001. Dynamic Process in surfactants stabilized Emulsion, Faculty of Chemistry, University of Sofia.

Di Terlizzi, S.D., 1994. Introduction to coagulation and flocculation of waste water. Environment System Project, USA,

Edzwald, J.K., 1987. Coagulation-sedimentation-filtration process for removing organic substances from drinking water: Control of organic substances in water and waste water. Noyes Data Corporation, Park Ridge, New Jersey.

Fernandez-Kim, S., 2004. Physiochemical and Functional Properties of Crawfish Chitosan as Affected by Different Processing Protocols. M.Sc. Thesis, Louisiana State University, U.S.A.

Fridrikhsberg, D.A., 1984. A course in Colloid Chemistry. Mir Publishers Moscow.

Greenberg, A.E., 1992. Standard Method for the Examination of Water and Waste Water. APHA and AWWA. 18th Edn. Washington, D.C, USA.

Holthof, H., S.U. Egelhaaf, M. Borkove, 1996. Coagulation Rate measurement of colloidal particles by Simultaneous Static and Dynamic light Scattering. Langmuir. American Chemical Society.

Jin, Y., 2005. Use of a high Resolution Photographic Technique for the studying of Coagulation/ flocculation in water treatment. M. Sc thesis, University of Saskatchewan, Saskatoon, Canada.

Joint America Water Works Association (JAWWA), 1985. Standard Methods for the examination of Water and Waste Water, USA.

Ma, J.J., G. Li, G.R. Chen, G.O. Xu and G.Q. Cai, 2001. Enhanced Coagulation of surface waters with high organic content by permanganate preoxidation. Water Science and Technology. Water Supply, 1 (1): 51 - 61. China.

Metcalf and Eddy, 2003. Physical Unit Process, Waste Water Engineering Treatment and Reuse. 4th Edn. Tata-McGraw Hill. New York.

Nicholls, H.A., 1979. Orthogenetic flocculation of phosphate precipitate in a multi-compartment reactor with non-ideal flow. Prog. Water Technol., pp: 61-88. Pergamon Press.

O'Melia, C.R., 1978. Coagulation in waste water treatment: The scientific basis of flocculation, (NATO Advanced Study Inst. Series, Series E, Appl. Sc. No 27) In: Ives, K.J. (Ed.). Sijthof and Noordhoff, Alpenan den Rijn, Netherlands.

Smoluchowski, M., 1917. Versucheiner Mathematischen Theorie der Koagulations Kinetic Kolloider Lousungen. Z. Phys. Chem., 92: 129-168.

Van-Zanten, J.H. and M. Elimelechi, 1992. Determination of Absolute Coagulation Rate Constant by Multi light Scattering. J. Coll. Interface Sci. USA., 154 (1).

Water Science Technology (WST), 2005. About Coagulation and flocculation. Information Bulletin, U.S.A.